Temporal Sequence and Spatial Distribution of Early Events of Fertilization in Single Sea Urchin Eggs

ANDREW EISEN, DANIEL P. KIEHART, STEVEN J. WIELAND, and
GEORGE T. REYNOLDS
The Marine Biological Laboratory, Woods Hole, Massachusetts; The Children's Hospital of Philadelphia,
Pennsylvania; The Department of Cell and Developmental Biology, Harvard University, Cambridge,
Massachusetts; The Department of Anatomy, Hahneman University, Philadelphia, Pennsylvania; and The
Department of Physics, Princeton University, New Jersey

ABSTRACT Measurements and observations of five early events of fertilization, singly and in pairs, from single sea urchin eggs have revealed the precise temporal sequence and spatial distribution of these events. In the *Arbacia punctulata* egg, a wave of surface contraction occurs coincident with membrane depolarization ($t = 0$). These two earliest events are followed by the onset of a rapid, propagated increase in cytoplasmic-free calcium at ~23 s as measured by calcium-aequorin luminescence. The luminescence reaches its peak value by 40 s after the membrane depolarization. The luminescence remains uniformly elevated for some time before its decay over several minutes. The onset of an increase in the pyridine nucleotide (NAD(P)H) fluorescence follows the membrane depolarization at ~51 s. The fertilization membrane begins its elevation in a wave-like fashion coincidentally with the increase in NAD(P)H fluorescence. Similar results are observed in the *Lytechinus variegatus* egg.

The results suggest that while the increase in cytoplasmic-free calcium may be important for many changes occurring in the egg, the elevated-free calcium is not directly responsible for the propagated wave of cortical granule exocytosis.

Fertilization initiates various physiological, biochemical, and structural changes within the egg that occur in a well-orchestrated manner both temporally and spatially. These events are requisite for normal embryonic development (8, 9). Included among the early events of fertilization are sperm-egg fusion, membrane depolarization, a surface contraction, an increase in cytoplasmic free calcium, the exocytosis of cortical granules, and a change in the pyridine nucleotide redox state. To some extent the sequence of these early events is known (8, 12, 19, 26).

That we might better understand the significance and casual relationships among the various events, we have examined simultaneously several of the events that occur within single sea urchin eggs at fertilization. The use of single eggs allows for the precise determination of the sequence of events which is unobtainable from studies that employ a population of eggs. Specifically, we have examined the temporal and spatial relationships among the fertilization potential, surface contraction, increase in cytoplasmic free calcium, NAD(P)H fluorescence, and elevation of the fertilization membrane.

The relationships among the various early events have been largely inferential although some work has been reported from single cells (12, 25, 26). We are principally concerned with when the increase in cytoplasmic-free calcium occurs relative to the other events. The increase in cytoplasmic-free calcium has been associated with sperm-egg fusion, initiation of the fertilization potential, the surface contraction, and, of course, the cortical reaction and fertilization membrane elevation (4, 8-11, 18, 20, 28, 29, 32). A precise determination of the temporal sequence of the early events in single eggs would help clarify the role, if any, for calcium in each of the other events.

We find that the fertilization potential ($t = 0$) is followed by an increase in intracellular-free calcium beginning at 23 ± 3 s ($n = 3$) and the redox state of the pyridine nucleotides becomes more reduced (fluorescent) at 51 ± 7 s ($n = 3$) in the *Arbacia punctulata* egg. Further, we spatially resolve the distribution of both the calcium increase and the redox change and demonstrate that each occurs with a cytoplasmic distribution. Finally we note that the fertilization membrane begins

its elevation coincidentally with the change in the NAD(P)H redox state. Less extensive measurements from eggs of *Lytechinus variegatus* are qualitatively similar.

MATERIALS AND METHODS

Gametes were shed from *A. punctulata* and *L. variegatus* by electrical stimulation or intracoelemic injection of 0.5 M KCl. Eggs were washed twice in artificial or filtered natural sea water. Eggs were immobilized, compressed, and slightly flattened, between parallel coverslips in a chamber designed for microinjection (16). Freshly diluted sperm were added to the chamber in the dark through a micropipette positioned some distance away from the egg. Sperm have access to the egg in a restricted equitorial distribution. Experiments were conducted at room temperature (18–20°C).

Aequorin or acetylated aequorin, a sensitive and specific calcium-photoprotein (3, 29, 30), was pressure injected into a single 75-μm diam *A. punctulata* or 120-μm diam *L. variegatus* egg for each experiment. In *A. punctulata* 14 pl of the aequorin solution was injected (10 mg/ml in 50 mM HEPES, 0.2 mM EGTA, pH 6.9–7.0). It was found that HEPES buffer was tolerated better on injection into the cells than others that were tried. The inclusion of EGTA in the injection buffer protected the aequorin from accidental contamination and led to light signals higher than those from chelator-free preparations (5). The acetylated aequorin was used in later studies where both the temporal and the spatial dynamics of the calcium transient were investigated as it has a higher photon yield than the native protein (30). The final concentration of aequorin in the injected *A. punctulata* egg was ~13 μm.

For the detection of the calcium-aequorin luminescense, light collected by an "objective" (Nikon ×24/1.15 NA condenser, Zeiss ×25/0.8 NA, Zeiss ×25/0.6 NA, Leitz × 50/1.0 NA) was directed to either a photomultiplier or an image intensifier. An EMI 6256 SA photomultiplier was operated at −1,100 V and had a dark current of ~10 pA. The output was amplifed with a Kiethley electrometer and the current recorded on a Gould chart recorder. The output of the EMI four-stage, magnetically focused image intensifier (9912) was observed in real time with a Dage silicon-intensified target (SIT) vidicon and recorded on video tape. Alternately the image tube output cold be directly photographed using high speed (ASA 10,000) Polaroid film.

Electrophysiologic measurements were made with a 3 M KCl-filled glass electrode (~100 Mohms) connected to a WPI M701 amplifier. The sea water bath in the Lucite chamber was grounded through a seawater-agar/Ag(Cl)$_2$ /Ag wire.

The 450 nm NAD(P)H fluorescence (5, 8) was stimulated by monochromatic 365 nm light attenuated with neutral density filters such that bleaching was reduced to <15% under continuous excitation (5). The fluorescence was measured with the photomultiplier tube noted above.

Photographs of the eggs before and after fertilization were taken by conventional photomicrography. Analysis of both the temporal and spatial dynamics of the calcium transient was accomplished by photographing the video monitor during video playback for successive 1-s intervals with ~¼ s between exposures for automatic advancement of the film. The photographs could be subsequently analyzed by densitometry. Alternatively light guides have been placed against the video monitor overlying various positions of the image of the egg and the light directed to a photomultiplier. Fig. 1 presents a schematic of the experimental system and Fig. 2 demonstrates how the video images can be analyzed.
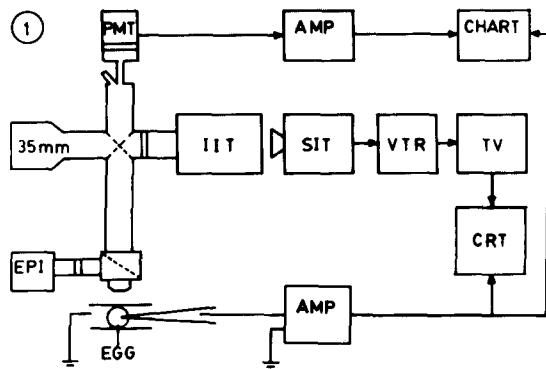

Figure 1   System schematic. The experimental system consists of a microscope with a DC-regulated Hg arc epi-fluorescence (EPI) attachment, low-noise/high-gain photomultiplier tube (PMT), and image intensifier tube (IIT), silicon intensified target vidicon (SIT), and with various amplifiers (AMP) and recording devices to obtain temporal and spatial records of the fluorescent or luminescent changes occurring within a single egg.

Experimental Design: We wished to examine the temporal and spatial relationships of various early events of fertilization not all of which could be measured or observed simultaneously. The individual events have been studied in several hundred, single eggs. For studies of multiple events the membrane depolarization served as a temporal reference point. It is one of the earliest measureable changes that occurs at fertilization and it occurs over a far shorter period of time (~100 ms) relative to many other changes (13, 26). We have taken the membrane depolarization as $t = 0$.

With care it is possible to first inject a single egg with aequorin and then follow with impalement by a microelectrode such that an undamaged membrane potential in the range of −75 to ~−125 mV is obtained (13, 14, 21). We were able to obtain simultaneous measurements of both the potential change and the simultaneous measurements of both potential change and the calcium transient that follows from three *A. punctulata* eggs. The results are summarized in Table I. Likewise, in a separate set of experiments we were able to obtain simultaneous measurements of both the membrane potential and the change in NAD(P)H fluorescence from three *A. punctulata* eggs. The results are summarized in Table II.

RESULTS

Timing of Early Events in Arbacia punctulata

Fig. 3 is a composite of representative records from two eggs. In one egg both the membrane potential (*a*) and the
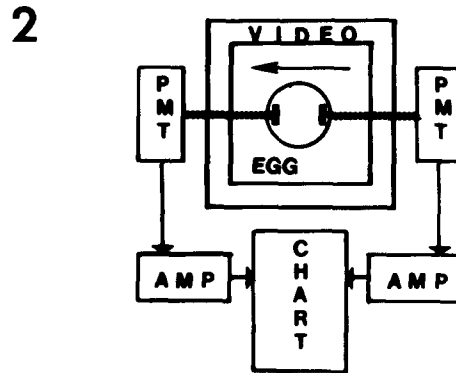

Figure 2   Video measurements. Determination of the propagation time of the calcium transient is accomplished by measuring the onset of luminescence from opposite ends of the video image of the egg. Light pipes (striped) collect the light that is measured by two uncalibrated PMTs. The amplified signals are displayed on a dual channel chart recorder.

Table I

Onset of the Calcium Transient after the Onset of the Fertilization Potential

Egg	Membrane potential	Transient onset
	mV	s
A	−75	21
B	−80	21
C	−90	28
D	−15	23
E	−50	28

Table II

Onset of the NAD(P)H Fluorescence Change after the Onset of the Fertilization Potential

Egg	Membrane potential	Fluorescence change onset
	mV	s
F	−80	60
G	−100	42
H	−120	51
I	−10	53
J	−40	66

3a

b   CALCIUM

c   NAD(P)H

SC   FM

```
    ▼      ▼      ▼
|    30     60     90    120    150    180    s
```
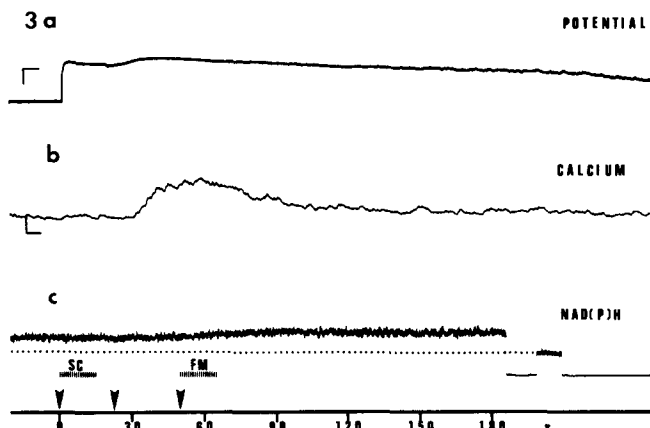
FIGURE 3 Early events of fertilization. This is a composite of records from two *A. punctulata* eggs showing the temporal relationships among the membrane potential (a), calcium transient (b), change in NAD(P)H fluorescence (c), and two structural changes—the surface contraction (SC) and the fertilization membrane elevation (FM). Bars in a mark 0 mV (horizontal) and −41 mV (vertical). Bars in b mark 0 pA (horizontal) and 14 pA (vertical). The dotted line in c marks the background fluorescence due to the optical system with the signal from the egg above the dotted line.

calcium transient (calcium-aequorin luminescence) (*b*) were measured simultaneously. In the other egg the membrane potential (not shown) and the NAD(P)H fluorescence (*c*) were measured simultaneously. With the membrane depolarization taken as $t = 0$, the calcium transient began at 23 ± 3 s ($n = 3$) and the NAD(P)H fluorescence increase began at 51 ± 7 s ($n = 3$). Similar time intervals between membrane depolarization and the calcium transient or the fluorescence change were also obtained from eggs with a less negative potential but are not included in the average values but are included in the tables (5, 7). Simultaneous observations of many single eggs with monochromatic green (546 nm) light during measurements of the blue (450 nm) NAD(P)H fluorescence revealed that a surface contraction begins at about the time of the membrane depolarization and that the fertilization membrane begins its elevation at the time of the NAD(P)H fluorescence increase. The NAD(P)H fluorescence change is quite small in the *A. punctulata* (and *L. variegatus*) egg compared with the fluorescence change found in the eggs from other species of sea urchins (5, 6). Details of the change in pyridine nucleotide fluorescence will be presented elsewhere.

Calcium Transient Calibration

Precise determinations of the intracellular calcium concentration using aequorin are difficult but possible. They require knowledge of the cytoplasmic concentrations of cations such as potassium and magnesium as well as estimate of the pH (1, 3, 29). Allen and Blinks (1) devised a calibration scheme that compares the maximum light output during a physiologic event to the maximum light output after exposure to a saturating amount of calcium. We have duplicated this scheme using our particular preparation of aequorin and optics. In this fashion the magnitude of the calcium transient is compared with the signal obtained from aequorin injections into Ca/Mg/EGTA buffers. The free calcium concentration of the buffers was calculated according to Portzehl (22) by Dr. E. D. Salmon (University of North Carolina). At least three measurements were made for each calcium concentration and 14 measurements of the calcium transient were made with the
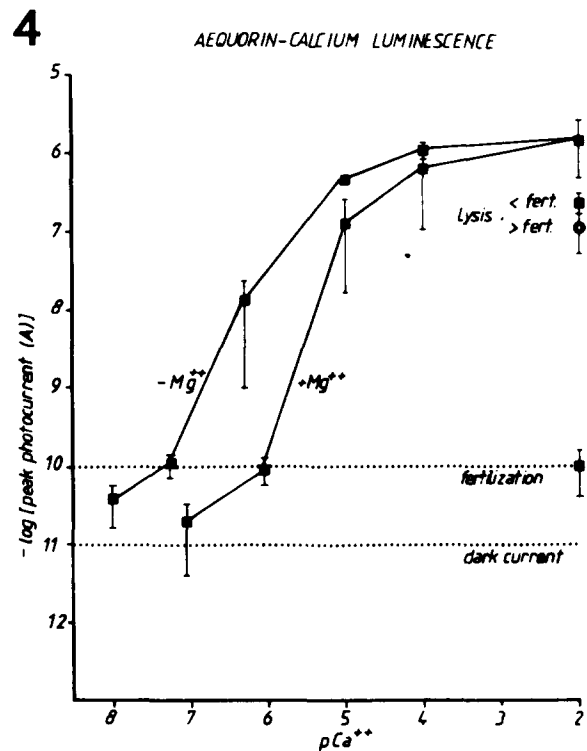
4

FIGURE 4 Calibration curves. The aequorin preparation used in one series of studies on eggs from *A. punctulata* was injected into the experimental chamber containing EGTA-buffered $Ca(Cl)_2$ solutions (pH 6.9) in presence or absence of 0.5 mM Mg^{++}. The peak luminescence is plotted as a function of pCa. The signal due to fertilization and the PMT dark current are indicated. The signal from a single fertilizing egg corresponds to ~1.0 μM free calcium when magnesium is present. The peak signals before and after fertilization from single, aequorin-injected eggs lysed with Triton-X-100 in sea water are also indicated. The total light output from the lysed eggs is comparable to the light output from aequorin injections directly into sea water. The peak value is lower due to slow mixing in the lysing egg.

same sample of aequorin. The calibration curves presented in Fig. 4 were obtained using the same amount of aequorin that was injected into single eggs. The error bars are one standard deviation and are asymmetric due to the logarithmic plot.

We detected no resting luminescence either with the photomultiplier or with the image intensifier system from the unfertilized, aequorin-injected eggs from both *A. punctulata* and *L. variegatus*. This suggests that the resting level of free calcium is <0.1 μM. Interpolation of the fertilization signal from 14 single eggs injected with the same preparation of aequorin onto the calibration curve generated in the presence of a physiologic amount of magnesium indicates that the fertilization signal results from a transient of ~1 μM of free calcium. Our calibration buffers were of low ionic strength and may therefore lead to a low estimate of both limits. Our estimates are in accord with the estimates of other investigators of the calcium transient in sea urchin and other eggs and the threshold for cortical granule exocytosis (2, 9–11, 17, 31, 32).

Spatial Distribution of the Calcium Transient

The release of calcium from its intracellular source resulted in luminescence from the reaction of calcium with the exogenous cytoplasmic aequorin. The amount of light coming from a single aequorin-injected sea urchin egg is quite small:

a countable number of photons. To see where the light originates requires the use of image intensification techniques (23, 24). The images produced by the image intensification methods from these photon-limited events appeared speckled and were not continuous in intensity. Each spot is the result of a single photon generated by the intracellular calcium-aequorin reaction.

Thus the temporal dynamics of the spatially varying calcium transient depend greatly upon the photon yield from the intracellular calcium-aequorin reaction and the ability to collect and record the emitted photons. During the course of these studies from 1977–1983 significant improvements in the photon yield, of light collection, and in recording devices have occurred and the evolution of the results will be described.

The first experiments were performed with eggs from the sea urchin L. variegatus using an aequorin preparation containing 3 mg/ml of protein in a PIPES-containing buffer (5). The eggs were injected with 3-6% of their volume of the aequorin solution. Light was collected with a × 25/0.65 NA microscope objective and directed to the image intensifier tube. The photon yield was sufficiently low that real-time video records of the image tube output screen could not be obtained with the video camera then available. However by integrating the image tube output photographically with high-speed film (Polaroid 10,000 ASA) for various lengths of time we were able to record the calcium transient at fertilization. An example of these results is presented in Fig. 5. We see the distribution of luminescence from two L. variegatus eggs. The exposure times were 5 s, 5 s, and 40 s in a–c, respectively. Approximately 1–2 s elapsed between exposures. Of the two eggs, the upper egg appears to be uniformly luminescent within the time of the first exposure (5 s) while the bottom egg appears to be uniformly luminescent within the time it took to advance the film and take the second exposure (2 + 5 s). The luminescence persisted for several minutes and decayed in a fairly uniform manner (17).

This result was something of a surprise. It differed appreciably from the result that was obtained on this instrument from eggs of the Medaka (10). In the egg from the Medaka a restricted region of elevated cytoplasmic calcium propagates across the egg with a similar time course to the cortical reaction/fertilization membrane elevation. In the egg from L. variegatus the entire cytoplasm appeared to be uniformly luminescent within 5-7 s. This is a considerably shorter period of time than for the propagated cortical reaction/fertilization membrane. The fertilization membrane elevates in a propagated fashion in the egg of L. variegatus, in ~24 s (17). Thus,

if there is a propagated wave of elevated cytoplasmic calcium in the sea urchin egg it occurs more quickly than the propagated wave of the cortical reaction/fertilization membrane elevation.

The precise temporal dynamics of the calcium transient awaited our acquisition of a SIT vidicon which enabled us to view the calcium transient through the microscope-image intensifier system in real-time. These real-time studies, begun in 1981, of the calcium transient at fertilization were done with eggs from the sea urchin A. punctulata. The egg from A. punctulata is smaller than the egg from L. variegatus and it is pigmented. Both of these features will decrease the photon yield from the intracellular calcium-aequorin reaction. Nonetheless these studies were undertaken because of the ability to centrifugally stratify the organelles in the living, single, A. punctulata egg; which would be useful in dissecting the origin of the calcium transient (5). Such experiments have been done and will be described in detail elsewhere.

The initial studies of the real-time dynamics of the calcium transient in the normal, uncentrifuged A. punctulata egg were disappointing. Because the photon yield was sufficiently low it required temporal integration of the video record for 5-10 s to generate an image (5). This was unacceptably long to determine the dynamics of any propagated wave of elevated free calcium.

A significant improvement in the temporal and spatial resolution of the calcium transient was brought about by the development of an acetylated aequorin by Dr. O. Shimomura (Marine Biological Laboratory Woods Hole, MA [30]). In our hands this preparation had a 3-30 times greater photon yield than the native protein; comparable with reported values (30). As a consequence the temporal resolution improved by a corresponding factor.

We present two examples in Figs. 6 and 7 of the calcium transient at fertilization in single, normal A. punctulata eggs that had been injected with acetylated aequorin. In each panel of the figures there is a sequence of five photographs taken for 1 s each of the video monitor during play back of the real-time video records. Approximately ¼–½ s in time separates each exposure to accommodate the automatic advancement of the film. It is now apparent that there is indeed a propagated wave of elevated cytoplasmic calcium during fertilization of the sea urchin egg. The propagation time determined from the photographs is 6–9 s.

The propagation time can also be determined from direct measurements. The luminescence that originates from opposite ends of the image of the egg on the video monitor can be detected with light pipes connected to photomultiplier tubes. The propagation time is determined when the light pipes are placed across the image of the egg on the video monitor in the direction of the propagated response. The propagation times for the two eggs shown in Figs. 6 and 7 are determined in this fashion from the photomultiplier traces shown in Figs. 8 and 9, respectively. It is interesting to note that the propagation time (6-10 s) is less than the average time to reach the peak luminescence (16.5 s; n = 30). Thus the luminescence signal is growing as the region of luminescence expands and for some time after the entire egg is luminescent.

The dynamics of the cytoplasmic calcium transient become more evident when presented in a slightly different form. A one-dimensional densitometric analysis of the individual photographs obtained from the real-time video record reveals both the expansion and growth of the luminescence. This was done with the video densitometer developed by Dr. J. C.

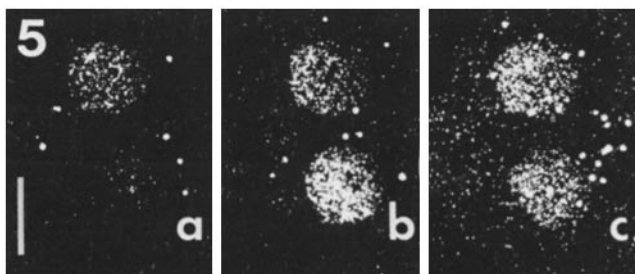
FIGURE 5 Calcium-aequorin luminescence in L. variegatus eggs. The panels show the distribution of calcium-aequorin luminescence (photons) from an IIT+Polaroid record of two L. variegatus eggs during successive (a) 5-, (b) 5-, and (c) 40-s intervals. Note the rapidity with which the bottom egg becomes uniformly luminescent. Bar, 130 μM. × 80.
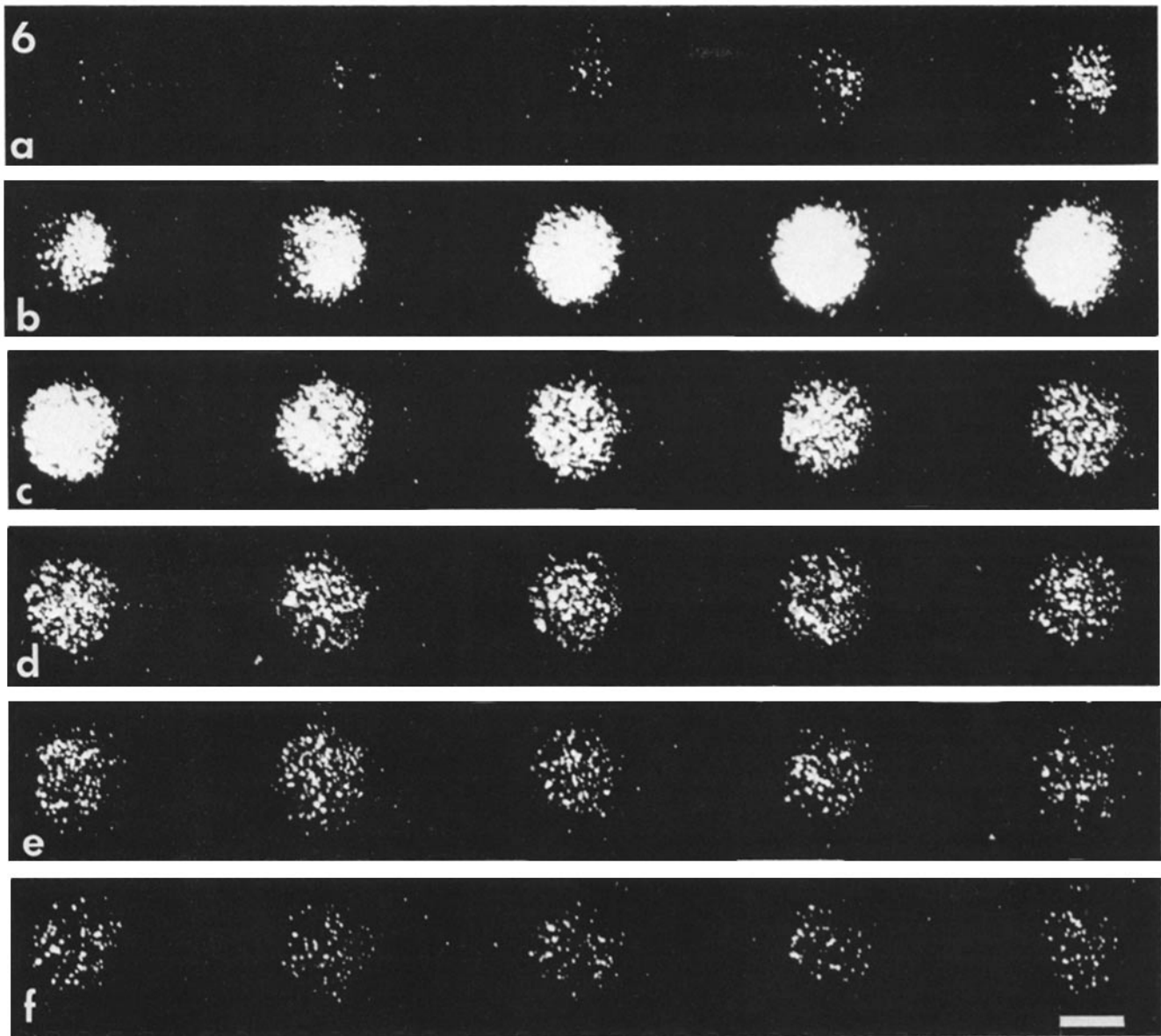
FIGURE 6 Calcium-aequorin luminescence in an *A. punctulata* egg. Each panel shows a sequence of five successive 1-s photographs taken of the video monitor during the playback of the real-time record of the calcium transient in a single, acetyl aequorin-injected *A. punctulata* egg. The photographs are continuous throughout the figure. Note that the transient begins on the right side of the egg and traverses the egg in ~6 s. The luminescence decays uniformly. Bar, 50 μM. × 200.

Haselgrove (Department of Biophysics, University of Pennsylvania; Philadelphia). Results are presented in Fig. 10 of the analysis for the egg of Figs. 6 and 8. In Fig. 10 *a* are superimposed densitometer traces of exposures 4–9 of Fig. 6. The arrowheads at the bottom of Fig. 10 *a* mark the advancing edge of the calcium transient (from right to left). Note also how the luminescence increases while the region of luminescence expands. In Fig. 10 *b* are superimposed densitometer traces of exposures 9–13 of Fig. 6. The luminescence decreases uniformly. The inset in Fig. 10 *b* shows how the densitometer traces are obtained: The density of the film (luminescence) in a band (striped) that crosses the egg perpendicularly to the direction of the calcium transient (arrow) is plotted against the position across the egg.

DISCUSSION

The principal aim of these studies was to determine more precisely the temporal and spatial relationships among several

of the early events of fertilization. We were particularly interested in when and where the transient increase in cytoplasmic-free calcium occurs because calcium has been associated with a multitude of physiologic processes. Through observations and measurements of single and simultaneous events in many single eggs from the sea urchin *A. punctulata* we can now comment upon the role for calcium in the fertilization potential, surface contraction, cortical reaction/fertilization membrane elevation, and change in the NAD(P)/NAD(P)H redox state.

A proviso in the discussion that follows relates to our ability to detect cytoplasmic-free calcium with aequorin. Based on our microscope-photomultiplier system calibration curves the limit to detection is at or slightly below 0.1 μM in the presence of magnesium. With the microscope-image intensifier system, because of the improved signal-to-noise characteristics of an area detector, small, localized changes in cytoplasmic-free calcium would not be missed whereas they might get buried
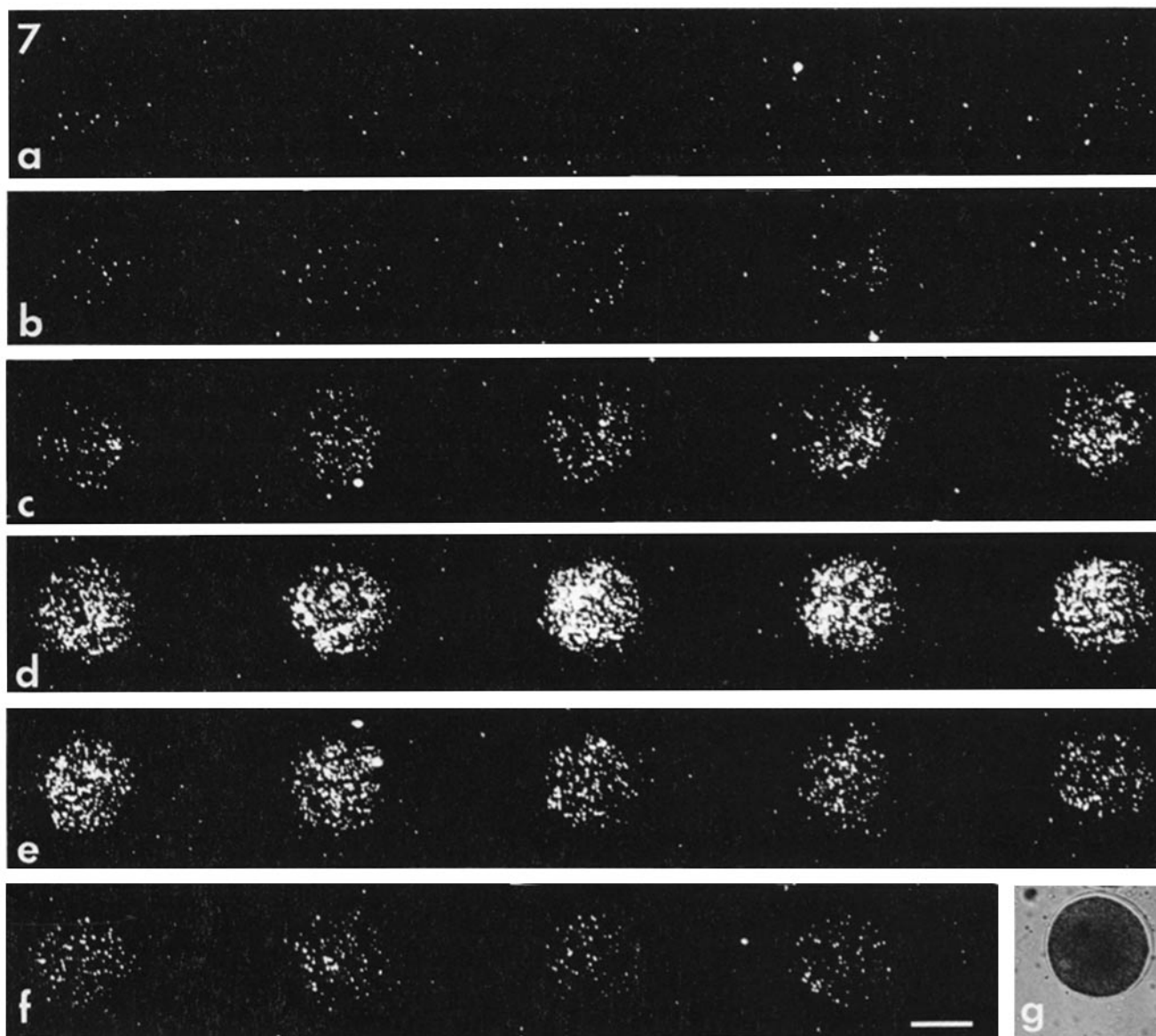
FIGURE 7   Calcium-aequorin luminescence in an *A. punctulata* egg. This figure is similar to the previous figure and demonstrates the propagated calcium transient in another single *A. punctulata* egg. The egg following the calcium transient with its elevated fertilization membrane is shown in g. Bar, 50 μM. × 180.

within the photomultiplier noise. Using both systems we detect no resting luminescence from the aequorin-injected unfertilized egg. In addition we detect no resting luminescence with either system using the more active acetylated aequorin. We are confident, therefore, that the resting level of free calcium is <0.1 μM and that we can detect any increase above that level in the *A. punctulata* egg during the early events of fertilization.

The fertilization potential is one of the earliest demonstrable changes that occur in the egg upon insemination. Calcium could be involved in its initiation as has been suggested for *Rana pipiens* (4) or golden hamster eggs (18). Our data suggests otherwise in the sea urchin egg as the fertilization potential is initiated over 20 s prior to the first detectable change in cytoplasmic-free calcium.

Fusion of the sperm and egg has been reported to occur 1–4 s after the onset of the fertilization potential in eggs from the sea urchin *L. variegatus* (26). It has been suggested that the sperm acts as a calcium "bomb" which then initiates a

calcium-dependent calcium release from sources within the egg (15). If sperm-egg fusion occurs with similar rapidity after the fertilization potential in eggs from *A. punctulata*, it occurs significantly before any detectable change in cytoplasmic-free calcium. Thus the notion of a calcium "bomb" needs to be modified.

Following adherence of the fertilizing sperm and sperm-egg fusion a surface contraction occurs (5, 30). The mechanism of this contraction is unknown but may be due to mechanical, osmotic, or other forces (27, 32). A mechanical mechanism based on the extensive meshwork of actin filaments in the egg cortex is an attractive possibility. Given the well-defined role for calcium in actin-myosin contractile systems it seems doubtful that such a system is invoked for the surface contraction as it, too, precedes any detectable change in cytoplasmic-free calcium.

The calcium transient itself begins at the point of insemination and propagates across the egg quickly. The calcium-aequorin luminescence increases and spreads simultaneously
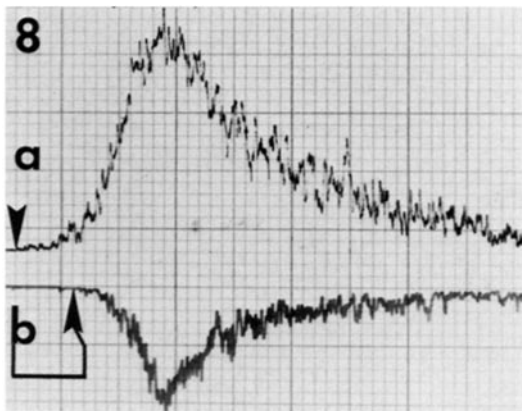
FIGURE 8 Propagation time. The propagation time for the calcium transient for the egg shown in Fig. 6 is determined by the method shown in Fig. 2. Trace *a* is the luminescence from the point of origin. Trace *b* is the luminescence from the opposite pole of the egg. The two traces are displaced one small division from each other and the bracket indicates a propagation time of 6 s. Each small horizontal division is 1 s. The luminescence is displayed vertically on an arbitrary scale.
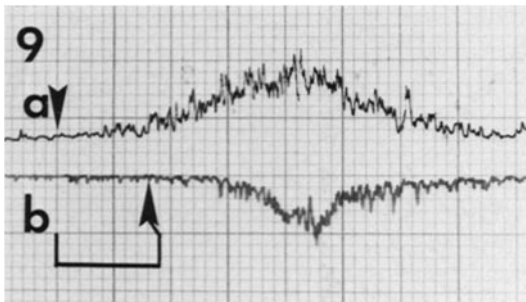

FIGURE 9 Propagation time. This figure is similar to the previous figure. The propagation time for the egg shown in Fig. 7 is determined from the traces to be 9 s.
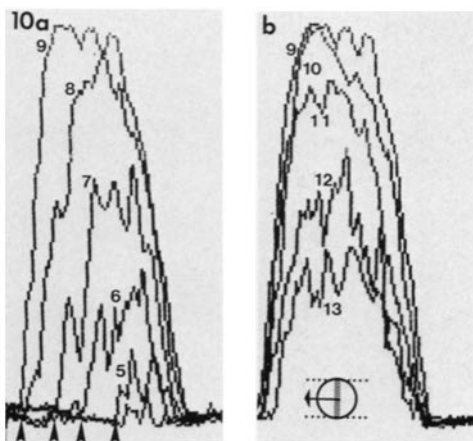

FIGURE 10 Luminescence distribution changes with time. A densitometric analysis of the photographs in Fig. 6 are presented during the propagation and growth of the luminescence (a) and during the decay of the luminescence (b). The numbers refer to the exposure in the sequence of Fig. 6. See the text for details.

and then continues to increase. It stays at its peak value for a variable period of time (from 3 to 30 s) and then decays uniformly over several minutes.

In the *A. punctulata* egg the calcium transient is first de-

tected ~23 s after the fertilization potential and reaches its peak value ~17 s later; 40 s after the fertilization potential. The fertilization membrane begins its elevation at ~51 s after the fertilization potential. Thus, on average, there is a delay of ~11 s between reaching the peak cytoplasmic-free calcium concentration and the onset of fertilization membrane elevation. What accounts for this delay?

Two causes for the delay come to mind immediately. The first is that the delay is accounted for by a delay between cortical granule exocytosis and the membrane elevation. The second is that the delay is accounted for by a delay between the attainment of a threshold calcium concentration and cortical granule exocytosis with simultaneous fertilization membrane elevation. A contribution from each mechanism may be involved and it may be difficult to separate the delay into its component parts (27). However, data from two investigations suggests that the delay is associated with the first mechanism—a delay between exocytosis and fertilization membrane elevation.

The first investigation was by Moser in 1939 (19). He observed that the cortical granules undergo exocytosis in a propagated fashion, which completely traverses the egg, prior to the fertilization membrane elevation. The time for this propagated response was 9.9 s at 25.7° C which is comparable to our delay time. This suggests that the propagated wave of exocytosis occurs during the time between the attainment of the peak, uniform cytoplasmic-free calcium concentration, and the fertilization membrane elevation.

The second investigation, by Jaffe et. al. (12), examined when the fusion of the cortical granules with the egg plasma membrane occurred following the fertilization potential. They measured the insertion of new, cortical granule-derived membrane into the egg plasma membrane in single sea urchin (*Strongylocentrotus purpuratus*) eggs by the change in membrane capacitance. They found that the capacitance began to change, on average, at 38 s after the fertilization potential. The onset of the capacitance change in that species coincides temporally with the attainment of the peak, uniform cytoplasmic-free calcium concentration in the *A. punctulata* egg (onset at 23 s + rise time of 17 s). This again suggests that the propagated wave of exocytosis occurs during the time between the attainment of the peak, uniform cytoplasmic-free calcium concentration and the fertilization membrane elevation.

Because the propagated wave of exocytosis seems to occur after the attainment of the peak, uniformly elevated cytoplasmic-free calcium this implies that the change in cytoplasmic-free calcium is not the direct cause of the propagated wave of exocytosis. Although an increase in cytoplasmic-free calcium may be necessary for exocytosis (2), the propagated wave of elevated cytoplasmic free calcium as well as the propagated wave of exocytosis are the consequence of some other substance or process that propagates across the egg. This substance or process remains to be discovered.

REFERENCES

1. Allen, D. G., and J. R. Blinks. 1979. The interpretation of light signals from aequorin-injected skeletal muscle cells: a new method of calibration. *In* Detection and Measurement of Free Ca^{++} in Cells. C. Ashley and A. Campbell, editors. Elsevier/North Holland, NY. 1979.
2. Baker, P. F., and M. J. Whitaker. 1978. Influence of ATP and calcium on the cortical reaction in sea urchin eggs. *Nature (Lond.).* 276:513–515.
3. Blinks, J. R., F. G. Prendergast, and D. G. Allen. 1979. Photoproteins as biological calcium indicators. *Pharmacol. Rev.* 28:1–93.
4. Cross, N. L. 1981. Initiation of the activation potential by an increase in intracellular calcium in the eggs of the frog, Rana pipiens. *Dev. Biol.* 85:380–384.
5. Eisen, A. 1982. Local intracellular metabolism at fertilization in single marine eggs. Thesis: University of Pennsylvania.
6. Eisen, A., and G. T. Reynolds. 1981. Source and behavior of the pyridine nucleotide fluorescence change in single, marine, invertebrate eggs. *Biol. Bull.* 161:335 a. (Abstr).
7. Eisen, A., G. T. Reynolds, S. J. Wieland, and D. P. Kiehart. 1983. Calcium transients during fertilization in single sea urchin eggs. *Biol. Bull.* 165:514 a. (Abstr.)
8. Epel, D. 1978. Mechanisms of activation of sperm and egg during fertilization of sea urchin gametes. *Curr. Top. Dev. Biol.* 12:185–246.
9. Gilkey, J. C. 1983. Roles of calcium and pH in activation of eggs of the Medaka fish, Orizayas latipes. *J. Cell Biol.* 97:669–678.
10. Gilkey, J. C., L. F. Jaffe, E. B. Ridgway, and G. T. Reynolds. 1978. A free calcium wave traverses the activating egg of the Medaka, Orizayas latipes. *J. Cell Biol.* 76:448–466.
11. Hagamuchi, Y., and Y. Hiramoto. 1981. Activation of sea urchin eggs by microinjection of calcium buffers. *Exp. Cell Res.* 134:171–179.
12. Jaffe, L. A., S. Hagiwara, and R. T. Kado. 1978. The time course of cortical vesicle fusion in sea urchin eggs observed as membrane capacitance changes. *Dev. Biol.* 67: 243–248.
13. Jaffe, L. A., and S. Hagiwara. 1979. Electrical properties of egg cell membranes. *Ann. Rev. Biophys. Bioeng.* 8:385–416.
14. Jaffe, L. A., and K. R. Robinson. 1978. Membrane potential of the unfertilized sea urchin egg. *Dev. Biol.* 62:215–228.
15. Jaffe, L. F. 1983. Sources of calcium in egg activation: a review and hypothesis. *Dev. Biol.* 99:265–276.
16. Kiehart, D. P. 1981. Studies on the in vivo sensitivity of spindle microtubules to calcium ions and evidence for a vesicular sequestering system. *J. Cell Biol.* 88:606–617.
17. Kiehart, D. P., G. T. Reynolds, and A. Eisen. 1977. Calcium transients during early development in echinoderms and teleosts. *Biol. Bull.* 153:335a. (Abstr.)
18. Miyazaki, S., and Y. Igusa. 1982. Ca-mediated activation of a K current at fertilization of golden hamster eggs. *Proc. Natl. Acad. Sci. USA.* 79:931–935.
19. Moser, F. 1939. Studies on a cortical layer response to stimulating agents. I. Response to insemination. *J. Exp. Zool.* 80:423–445.
20. Moy, G. W., G. S. Kopf, C. Gache, and V. D. Vacquier. 1983. Calcium-mediated release of glucanase activity from cortical granules of sea urchin eggs. *Dev. Biol.* 100:267–274.
21. Nuccitelli, R., and R. D. Grey. 1984. Review: controversy over the fast temporay block to polyspermy in sea urchins: a reevaluation. *Dev. Biol.* 103:1–17.
22. Portzehl, H., P. C. Caldwell, and J. C. Ruegg. 1964. The dependence of contraction and relaxation of muscle fibers from the crab Maia squinado on the internal concentration of free calcium ions. *Biochim. Biophys. Acta.* 79:581–591.
23. Reynolds, G. T. 1972. Image intensification applied to biological problems. *Q. Rev. Biophys.* 5:295–347.
24. Reynolds, G. T., and D. L. Taylor. 1980. Image intensification applied to light microscopy. *Bioscience.* 30:586–592.
25. Schatten, G. 1981. Sperm incorporation, pronuclear migration, and their relation to the establishment of the first embryonic axis: time-lapse video microscopy of the movements during fertilization of the sea urchin L. variegatus. *Dev. Biol.* 86:426–437.
26. Schatten, G., and D. Husler. 1983. Timing the early events during sea urchin fertilization. *Dev. Biol.* 100:244–248.
27. Schuel, H. 1978. Secretory functions of egg cortical granules in fertilization and development: a critical review. *Gamete Res.* 1:299–382.
28. Schmidt, T., C. Patton, and D. Epel. 1982. Is there a role for the calcium influx during fertilization of the sea urchin egg? *Dev. Biol.* 90:284–290.
29. Shimomura, O., F. H. Johnson, and Y. Saiga. 1962. Extraction, purification and properties of aequorin, a bioluminescent protein from the luminous hydromedusan, Aequora. *J. Comp. Physiol.* 59:223–239.
30. Shimomura, O., and A. Shimomura. 1982. EDTA-binding and acylation of the calcium-sensitive photoprotein aequorin. *FEBS (Fed. Eur. Biochem. Soc.) Lett.* 138:201–204.
31. Steinhardt, R. A., R. Zucker, and G. Schatten. 1977. Intracellular calcium release at fertilization in the sea urchin egg. *Dev. Biol.* 58:185–196.
32. Vacquier, V. D. 1981. Dynamic changes in the egg cortex. *Dev. Biol.* 84:1–26.